Differential cross sections of positron–hydrogen collisions*

Rong-Mei Yu(于荣梅)[1], Chun-Ying Pu(濮春英)[1], Xiao-Yu Huang(黄晓玉)[1], Fu-Rong Yin(殷复荣)[1], Xu-Yan Liu(刘旭焱)[1], Li-Guang Jiao(焦利光)[2], and Ya-Jun Zhou(周雅君)[3,†]

[1] *College of Physics and Electronic Engineering, Nanyang Normal University, Nanyang* 473061, *China*
[2] *College of Physics, Jilin University, Changchun* 130012, *China*
[3] *Institute of Atomic and Molecular Physics, Jilin University, Changchun* 130012, *China*

(Received 13 October 2015; revised manuscript received 15 January 2016; published online 27 May 2016)

We make a detailed study on the angular differential cross sections of positron–hydrogen collisions by using the momentum-space coupled-channels optical (CCO) method for incident energies below the H ionization threshold. The target continuum and the positronium (Ps) formation channels are included in the coupled-channels calculations via a complex equivalent-local optical potential. The critical points, which show minima in the differential cross sections, as a function of the scattering angle and the incident energy are investigated. The resonances in the angular differential cross sections are reported for the first time in this energy range. The effects of the target continuum and the Ps formation channels on the different cross sections are discussed.

Keywords: differential cross section, resonance, positron, hydrogen

PACS: 34.80.Uv **DOI:** 10.1088/1674-1056/25/7/073401

1. Introduction

The study of positron collisions with atoms has served as a fundamental testing ground for our understanding of particle and antiparticle interacting with atoms.[1] Due to its simplicity and fundamental importance, the positron collision with a hydrogen atom is very useful in the development of theoretical techniques for more complicated systems. One of the active areas in positron–atoms interactions, which has attracted considerable theoretical interest, is the resonances involving the positron.[2,3]

The resonances in positron–hydrogen scattering play an important role in the production of anti-hydrogen atoms through the rearrangement scattering of positronium by antiproton.[4–6] Even though there are not yet any reports of experimental observations, several theoretical methods have been used to demonstrate the existence of resonances in this system, including the method of complex-coordinate rotation,[7–9] the close-coupling method,[10–12] the hyperspherical close-coupling method,[13,14] the Harris–Nesbet variational method,[15,16] the stabilization method,[17–19] and the stochastic variational method.[20] However, most of these calculations are either limited to a specific one partial wave or constrained to resonance structures in total cross sections. In this work, we present resonances in angular differential cross sections and investigate the variation of the resonances along with the scattering angle. Theoretical study of differential cross sections is of great importance in collisional phenomena not only because the measurements are expressed by means of this quantity, but also because this quantity characterizes the details of the collisional dynamics. The nature of the differential cross section is generally characterized by its behavior around the critical points which are defined to the scattering angles at which the differential cross section has a deep minimum for specific incident energy. The critical points were first investigated by Buhring[21] in electron–atom systems. The author analyzed the origin of these critical points and demonstrated the same causations for positron and electron scatterings. Several methods have been used to investigate the existence of the critical points for positron–atom collisions. Wadhera *et al.*[22] predicted the existence of critical points for positron–rare-gas-atom collisions by using empirical relationships satisfied by the phase shift. Then Mandal *et al.*[23] and Ghoshal *et al.*[24] predicted the existence and the behavior of critical angles in elastic positron–hydrogen collisions using the state-of-the-art Schwinger variational method.

Comparing with a large number of previous works on the resonances in the positron–hydrogen system, only a few involve research on the resonance properties in angular differential cross sections. The studies of the angular dependence of the scattering cross section offer a special tool to investigate the resonances in more detail. In this work, our main object is to make a detailed study on the resonance features and the critical points of angular differential cross sections in positron–hydrogen scattering employing the momentum-space coupled-channels optical (CCO) method.[25] The CCO method for electron–atom collision given by McCarthy and Stelbovics[26] has been applied to calculate the energy-dependent phenom-

*Project supported by the Nanyang Normal University Science Foundation of China (Grant No. ZX2013017) and the National Natural Science Foundation of China (Grant Nos. 11174066, 61306007, and U1304114).

†Corresponding author. E-mail: zuolouzhoudx@163.com

© 2016 Chinese Physical Society and IOP Publishing Ltd

ena in electron–hydrogen scattering[27] and negative-ion resonances in electron–sodium[28] and electron–oxygen[29] systems. Good agreements with experiments and other calculations have been achieved. Recently, the CCO method for positron–atom scattering given by Zhou *et al.*[25] has been applied to study the energy-dependent phenomena in positron–atom systems.[30–34] In our previous work,[32,33] the energy-dependent phenomena and the resonance structures in the positron–hydrogen system have been studied in the framework of the CCO model. An equivalent local polarization potential has been used to describe the target ionization continuum and the positronium (Ps) formation rearrangement channels and therefore this method can ideally take the contributions of all reaction channels into account. The method has been applied to calculate various scattering cross sections (positronium formation, ionization, and total scattering cross sections) for the positron–hydrogen system and satisfactory results have been obtained comparing with experimental data and other theoretical calculations.[32,33]

2. Theoretical details

A detailed theoretical description of the CCO method has been given in the paper of Zhou *et al.*[25] and also in our previous work.[32–34] Here we outline the essential features of this method. The total scattering cross section is calculated by solving the momentum-space coupled-channels equations[26]

$$\begin{aligned}&\langle \boldsymbol{k}, i \mid T \mid 0, \boldsymbol{k}_0\rangle \\ &= \langle \boldsymbol{k}, i \mid V^{(Q)} \mid 0, \boldsymbol{k}_0\rangle + \sum_{j\in P}\int \mathrm{d}^3k' \langle \boldsymbol{k}, i \mid V^{(Q)} \mid j, \boldsymbol{k}'\rangle \\ &\times \frac{1}{E^{(+)} - \varepsilon_j - q'2/2}\langle \boldsymbol{k}', j \mid T \mid 0, \boldsymbol{k}_0\rangle. \end{aligned} \tag{1}$$

Here $\mid 0, \boldsymbol{k}_0\rangle$ and $\mid i, \boldsymbol{k}\rangle$ are the entrance and exit channel states, in which 0 and i represent the target states. The space of the target states has been divided into two parts, the P space consists of a finite set of discrete states including the entrance channel, and the Q space projects all the remaining discrete states and the continuum. $V^{(Q)}$ has two parts, the positron–target static potential V and the complex nonlocal polarization optical potential $W^{(Q)}$,

$$V^{(Q)} = V + W^{(Q)}. \tag{2}$$

Additionally, the optical potential $W^{(Q)}$ consists of two parts to describe the polarization effects of the target remaining discrete and ionization continuum and the positronium formation rearrangement, respectively. The form used here for the matrix element of the first part is

$$\begin{aligned}&\langle \boldsymbol{k}', i \mid W^{(Q)} \mid j, \boldsymbol{k}\rangle \\ &= \sum_{l\in Q}\int \mathrm{d}^3q \langle \boldsymbol{k}', i \mid V \mid l, \boldsymbol{q}\rangle \frac{1}{E^{(+)} - \varepsilon_l - q^2/2}\langle \boldsymbol{q}, l \mid V \mid j, \boldsymbol{k}\rangle \\ &+ \int \mathrm{d}^3q' \int \mathrm{d}^3q \langle \boldsymbol{k}', i \mid V \mid \psi^{(-)}(\boldsymbol{q}_<), \boldsymbol{q}_>\rangle \\ &\times \frac{\langle \boldsymbol{q}_>, \psi^{(-)}(\boldsymbol{q}_<) \mid V \mid j, \boldsymbol{k}\rangle}{E^{(+)} - q^2/2 - q'2/2}, \end{aligned} \tag{3}$$

where $\boldsymbol{q}_<$ ($\boldsymbol{q}_>$) represents the smaller (larger) one of $\boldsymbol{q}$ and $\boldsymbol{q}'$. In the present calculation, $\boldsymbol{q}_>$ is a plane wave with the corresponding momentum, while $\psi^{(-)}(\boldsymbol{q}_<)$ is a Coulomb wave orthogonalized to the initial target orbitals.

The optical potential describing the positronium formation is

$$\begin{aligned}&\langle \boldsymbol{k}', i \mid W_{\mathrm{Ps}}^{(Q)} \mid j, \boldsymbol{k}\rangle \\ &= \sum_n \langle \boldsymbol{k}', i \mid V \mid \widetilde{\chi}_n^{(-)}\rangle \frac{1}{E^{(+)} - \varepsilon_n - k_{\mathrm{Ps}}^2}\langle \widetilde{\chi}_n^{(-)} \mid V \mid j, \boldsymbol{k}\rangle, \end{aligned} \tag{4}$$

where

$$\mid \widetilde{\chi}_n^{(-)}\rangle = (1 - \mid i\rangle\langle i \mid) \mid \chi_n^{(-)}\rangle. \tag{5}$$

$\mid \widetilde{\chi}_n^{(-)}\rangle$ is required to be orthogonalized to the initial state of the hydrogen atom, i.e., $\mid i\rangle$, from which the electron is captured. $\mid \chi_n^{(-)}\rangle$ is the product of bound state of the positronium atom and the plane wave representing the motion of positronium center of mass. In Eqs. (3) and (4), we use an equivalent local approximation and make the angular momentum projection through

$$\langle \boldsymbol{k}', i \mid W^{(Q)} \mid j, \boldsymbol{k}\rangle = \sum_{l'', m''} i^{l''} C_{l'' \; l' \; l}^{m'' m' m} U_{l'' l' l}(K) Y_{l'' m''}(\hat{\boldsymbol{K}}), \tag{6}$$

where l, m and l', m' are the orbital angular momentum quantum numbers of the states i and j, respectively, $C_{l'' \; l' \; l}^{m'' m' m}$ denotes the Clebsch–Gordan coefficients, and the momentum transfer is written as

$$\boldsymbol{K} = \boldsymbol{k} - \boldsymbol{k}'. \tag{7}$$

For computation, we make the partial-wave expansion of the T and $V^{(Q)}$ matrix elements by defining the partial-wave matrix elements

$$\langle k' n' l' L' \parallel T_J \parallel L l n k\rangle \tag{8}$$

for total angular momentum J,

$$\begin{aligned}&\langle \boldsymbol{k}', n', l', m' \mid T \mid n, l, m, \boldsymbol{k}\rangle \\ &= \sum_{LML'M'JK} \langle k' \mid L'M'\rangle C_{L' \; l' \; l}^{M' m' k} \\ &\times \langle k' n' l' L' \parallel T_J \parallel L l n k\rangle C_{LlJ}^{Mmk} \langle LM \mid k\rangle, \end{aligned} \tag{9}$$

where $\langle k \mid LM\rangle \equiv Y_{LM}(k)$ and C_{LlJ}^{Mmk} is a Clebsch–Gordan coefficient.

The differential cross section for scattering from channel j to channel i at angle θ is

$$\frac{\mathrm{d}\sigma_{ij}}{\mathrm{d}\Omega} = (2\pi)^4 \frac{k_i}{k_j} \frac{\hat{S}^2}{\hat{l}^2} \sum_{m,m'} \left| \langle \boldsymbol{k}_i; n', l', m' \mid T \mid n, l, m; \boldsymbol{k}_j\rangle \right|^2, \tag{10}$$

where

$$\hat{l} = (2l+1)^{1/2}. \tag{11}$$

Once the scattering cross sections are obtained at various incident energies, the position and width of the resonance for a particular value of J can be obtained by fitting the Breit–Wigner formula with a linear background

$$\sigma_{\rm R} = \left| aE + b + \frac{c + {\rm i}d}{E - E_{\rm R} + 0.5{\rm i}\Gamma_{\rm R}} \right|^2 \tag{12}$$

to the partial cross section $\sigma_{\rm R}$ for each resonance over the resonance energy range. In the above fitting formula, E is the incident energy, and $E_{\rm R}$, $\Gamma_{\rm R}$, a, b, c, and d are the resulting fitting parameters. $E_{\rm R}$ is the resonance energy and $\Gamma_{\rm R}$ is the corresponding width.[28]

3. Results and discussion

In the present calculations, the P space consists of fifteen states, including 1s, 2s, 3s, 4s, 5s, 6s; 2p, 3p, 4p, 5p, 6p; 3d, 4d, 5d, 6d. The optical potentials describing the target ionization continuum are included in the channel couplings of 1s–1s, 1s–2s, 1s–2p. The optical potentials describing the positronium formation in the corresponding Ps($n = 1$) and $n = 2$ states are included in the above 1s–1s channel coupling. The optical potentials in other channel couplings have a small effect on the cross sections and therefore can be ignored. With the absence of any optical potentials, the normal close-coupling (CC) method is revisited.

We have done the calculations from 6.5 eV to 13.5 eV at an interval of 0.5 eV. In order to make an in-depth study of the angular differential cross section, we make use of surface plots. The results of the elastic differential cross sections are presented in Fig. 1. Some dramatic behaviors of the cross sections in the surface plots are shown. The differential cross section is highly peaked at 0° and the peak rises up with increasing incident energy. After it reaches the secondary maximum, the differential cross section decreases steadily at large scattering angles. At relatively high impact energies, the primary minimum and the secondary maximum which form a certain wave pattern appear to be prominent. The wrinkles in the surface plot of Fig. 1 clearly demonstrate such phenomena. The critical angle, lying upon the primary minimum, forms and changes slowly with varying incident positron energy. These critical points are formed due to the destructive interference of the scattered waves for different angular momentum states produced by the interaction between the positron and the hydrogen target. In Table 1, we list the critical angles along with the corresponding differential cross sections in elastic positron–hydrogen collisions at energies from 6.5 eV to 13.5 eV. In Fig. 2, the present results are compared with the calculations of Ghoshal and Mandal[24] obtained by the state-of-the-art Schwinger variational method when they are available. It is expected that the Schwinger variational method is more accurate in low energy elastic scatterings due to its variational consideration of all electron correlations in the intermediate scattering process and its calculation can be generally considered as the benchmark result to compare with. One can see that the present critical angles are in good agreement with their predictions, except at relatively high energies near the ionization threshold where our results are somewhat larger. We conclude that in such energy range, more excitation channels are open and the present CCO model with 15 physical states are not complete enough to represent the higher channel coupling effects. To get further information of the full differential cross sections predicted by the Schwinger variational method, the readers are referred to Fig.11 of Ref. [24] where the cross sections are plotted in log scale and the incident energies are represented by positron momenta. Generally, the dramatic behavior shown in the present differential cross sections has the same shape as well as magnitude as predicted by Ghoshal and Mandal.[24]

To have a transparent idea about the critical angles, we plot in Fig. 3 the differential cross sections as a function of the scattering angle for incident positron energies of 11.0 eV, 11.5 eV, 12.0 eV, and 12.5 eV. The results obtained with CC15 and CCO models are both present. In the CC15 model, no optical potentials are included. The critical angles obtained by the CC15 model are about 20°, while they are about 50° predicted by the CCO model in these energies. The critical angle decreases slowly with increasing incident positron energy in the CCO model, while it keeps steady in the CC15 model. Comparing with the results, it is noted that the effects of the target continuum and the Ps formation channels play an important role in shifting the critical angles and producing the correct differential cross sections.

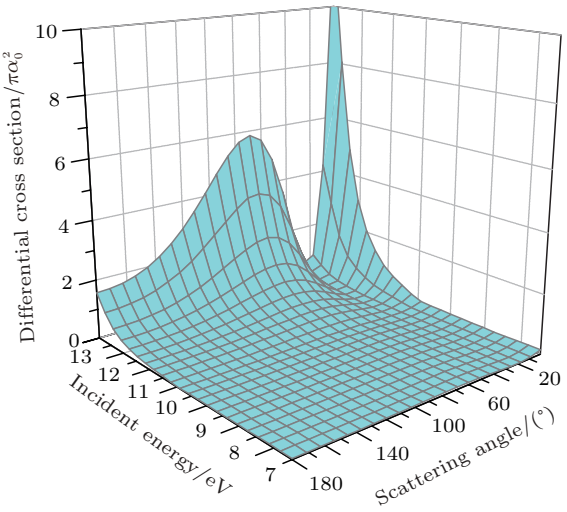


Fig. 1. (color online) The elastic differential cross section as a function of positron incident energy (6.5–13.5 eV) and scattering angle (0–180°).

Table 1. The critical angles and the corresponding differential cross sections in elastic positron–hydrogen collisions at incident positron energies from 6.5 eV to 13.5 eV.

Incident energy/eV	Critical angle/(°)	Differential cross section
4.9[a]	73.7[a]	0.0004[a]
6.5	67.21	0.00491
6.7[a]	65.8[a]	0.0020[a]
7.0	64.5	0.00400
7.5	62.3	0.00548
8.0	60.06	0.00503
8.5	58.4	0.00630
8.7[a]	55.8[a]	0.0055[a]
9.0	56.5	0.00540
9.5	54.9	0.00650
10.0	53.2	0.00680
10.5	52.5	0.00690
11.0	51.8	0.00625
11.0[a]	50.4[a]	0.0061[a]
11.5	50.56	0.00669
12.0	50.06	0.00639
12.5	49.66	0.00660
13.0	48.35	0.00694
13.5	47.21	0.00789
13.6[a]	44.3[a]	0.0060[a]
16.5[a]	39.5[a]	0.0074[a]

[a] The result of Ghoshal and Mandal.[24]

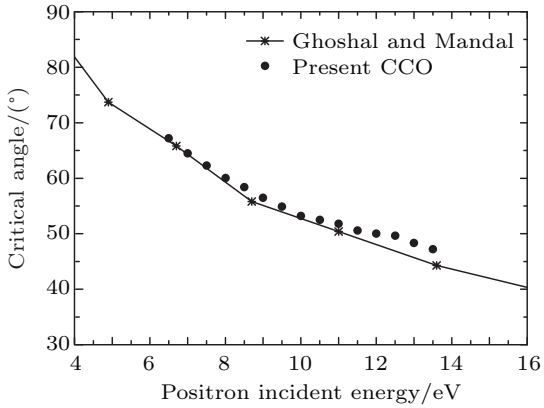


Fig. 2. Comparison of the present critical angles in elastic differential cross sections with the prediction of Ghoshal and Mandal.[24]

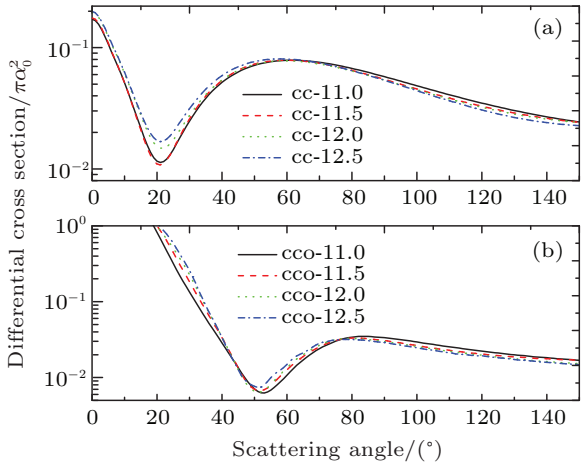


Fig. 3. (color online) The elastic differential cross sections as a function of scattering angle (0–150°) obtained by (a) CC15 and (b) CCO methods for positron incident energies of 11.0 eV, 11.5 eV, 12.0 eV, and 12.5 eV.

In our preceding paper,[32] we have reported the energy-dependent phenomena above the H($n = 2$) threshold for positron collisions with hydrogen in partial wave cross sections. The calculations are based on the CCO method and agree reasonably well with other available theoretical calculations such as those of Ho and Yan.[9] In this work, we perform the calculations at an interval of 0.001 eV in the vicinity of the resonance energy region and investigate the resonance structure in the angular differential cross sections. The results for selected angles of 50°, 80°, 135°, and 180° are shown in Fig. 4. The differential cross sections change rapidly as functions of the incident energy in the resonance region, where the resonance energies are indicated specifically. It is seen from Fig. 4 that the F-wave resonance at 12.570 eV is visible at all selected angles except 80°. The D-wave resonance at 12.652 eV and the I-wave resonance at 12.690 eV are absent at 50° and 135°, respectively. The other resonances including some high partial wave resonances manifest themselves at all selected angles. Besides these resonances, two peak features located at 12.241 eV and 12.276 eV are shown in the differential cross sections at the angle of 50°. Analyzing the results of the differential cross sections, we can find that the contributions of the same resonance are not monotonic at different scattering angles. This is probably because of the attractive dipole potentials, which result in the resonances that are not spherically symmetric.

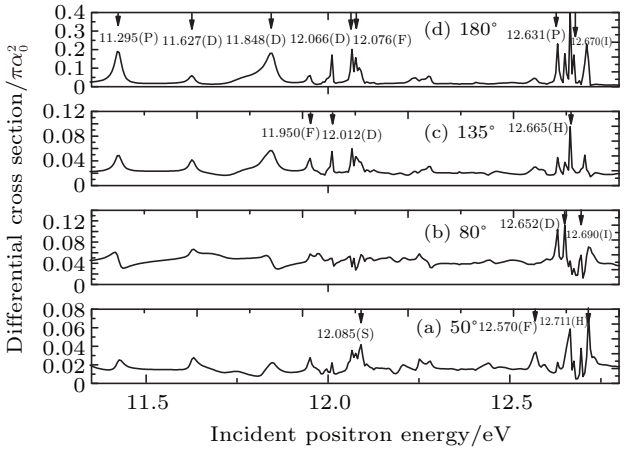


Fig. 4. The differential cross sections at (a) 50°, (b) 80°, (c) 135°, and (d) 180°. The positions of resonances are indicated by the arrows.

In order to investigate the effects of the target continuum and the positronium formation channels on the resonances, we have carried out the CC15 calculations. The results are shown in Table 2 and compared with the CCO calculations. All the resonances are confirmed in both models although slight discrepancies exist. Comparing with the results of the CC15 model, the resonance energies in the CCO model do not change much while the resonance widths are broadened. Such a result can be understood as a consequence of the fact that including the target continuum and the positronium formation

channels in the CCO model introduces additional decaying channels for the resonances. The lifetime of the resonances is shortened and the corresponding width is broadened, a result of the uncertainty principle.

Table 2. Comparison of resonance energies by CC15 and CCO models in e^+–H scattering. The E_R and Γ_R are in units of eV.

State	CC15		CCO	
	E_R	Γ_R	E_R	Γ_R
S	12.086	0.001	12.085	0.002
P	11.626	0.015	12.631	0.020
D	11.421	0.015	11.428	0.017
	11.846	0.017	11.848	0.021
	12.011	0.001	12.012	0.002
	12.066	0.003	12.066	0.004
	12.651	0.0001	12.652	0.0002
F	11.626	0.018	11.627	0.024
	11.951	0.011	11.950	0.010
	12.076	0.002	12.076	0.003
	12.566	0.015	12.570	0.020
H	12.666	0.0004	12.665	0.0005
	12.711	0.0003	12.711	0.0004
I	12.676	0.0002	12.670	0.0002
	12.691	0.0001	12.690	0.0001

4. Conclusion

We report some of the dramatic behaviors in the differential cross sections of e^+–H scattering. By using the momentum-space coupled-channel optical method, all reaction channels for positron–atom scatterings are included in the calculations with appropriate approximations. The critical points found in the angular differential cross sections are in good agreement with those reported by Ghoshal and Mandal.[24] The resonance structures are shown to have different structures at different scattering angles and further works are needed to shed more light on such phenomenon. The effects of the target continuum and the positronium formation channels on both the critical angles and the resonance parameters are investigated. It is shown that the contributions are very important in producing the correct shape of the differential cross sections and physically complete resonance width. It is hoped that our present work on resonances would provide useful information for future research.

References

[1] Charlton M and Humberston J M 2001 *Positron Physics* (Cambridge: Cambridge University Press)
[2] Ho Y K 2008 *Nucl. Instrum. Meth. B* **266** 516
[3] Ho Y K 1992 *Hyperfine Interactions* **73** 109
[4] Charlton M, Eades J, Horvath D, Hughes R J and Zimmermann C 1994 *Phys. Rep.* **241** 65
[5] Mitroy J and Stelbovics A T 1994 *Phys. Rev. Lett.* **72** 3495
[6] Mitroy J 1995 *Phys. Rev. A* **52** 2859
[7] Doolen G D, Nuttall J and Wherry C 1978 *Phys. Rev. Lett.* **40** 313
[8] Ho Y K and Yan Z C 2004 *Phys. Rev. A* **70** 032716
[9] Yan Z C and Ho Y K 2008 *Phys. Rev. A* **77** 030701
[10] Mitroy J and Stelbovics A T 1994 *J. Phys. B* **27** 3257
[11] Seiler G J, Oberoi R S and Callaway J 1971 *Phys. Rev. A* **3** 2006
[12] Mitroy J and Ratnavelu K 1995 *J. Phys. B* **28** 287
[13] Lin C D 1995 *Phys. Rep.* **257** 1
[14] Zhou Y and Lin C D 1995 *J. Phys. B* **28** 4907
[15] Gien T T 1995 *J. Phys. B* **28** L313
[16] Gien T T 1996 *J. Phys. B* **29** 2127
[17] Mandelshtam V A, Ravari T R and Taylor H S 1993 *Phys. Rev. Lett.* **70** 1932
[18] Kar S and Ho Y K 2005 *J. Phys. B* **38** 3299
[19] Roy U 2009 *Indian J. Phys.* **83** 1637
[20] Varga K, Mitroy J, Mezei J Z and Kruppa A T 2008 *Phys. Rev. A* **77** 044502
[21] Buhring W 1969 *Z. Phys.* **208** 286
[22] Wadehra J M, Stein T S and Kauppila W E 1984 *Phys. Rev. A* **29** 2912
[23] Mandal P, Kar S and Roy U 1998 *Nucl. Instrum. Meth. B* **143** 32
[24] Ghoshal A and Mandal P 2005 *Phys. Rev. A* **72** 042710
[25] Zhou Y, Ratnavelu K and McCarthy I E 2005 *Phys. Rev. A* **71** 042703
[26] McCarthy I E and Stelbovics A T 1983 *Phys. Rev. A* **28** 2693
[27] Stelbovics A T and Shang B 1992 *Phys. Rev. A* **46** 3959
[28] Jiao L, Zhou Y and Wang Y 2010 *Phys. Rev. A* **81** 042713
[29] Wang Y, Zhou Y, Jiao L and Ratnavelu K 2008 *Chin. Phys. Lett.* **25** 2027
[30] Liu F, Cheng Y, Zhou Y and Jiao L 2011 *Phys. Rev. A* **83** 032718
[31] Jiao L, Zhou Y, Cheng Y and Yu R 2012 *Eur. Phys. J. D* **66** 48
[32] Yu R, Cheng Y, Jiao L and Zhou Y 2012 *Chin. Phys. Lett.* **29** 053401
[33] Yu R, Zhou Y, Jiao L and Cheng Y 2012 *Chin. Phys. B* **21** 013404
[34] Yu R, Cheng Y, Wang Y and Zhou Y 2012 *Chin. Phys. B* **21** 053402